Physics Letters B 672 (2009) 354–360

Contents lists available at ScienceDirect

Physics Letters B

www.elsevier.com/locate/physletb

Higgs boson pair production at a photon–photon collision in the two Higgs doublet model

Eri Asakawa [a], Daisuke Harada [b,c], Shinya Kanemura [d,*], Yasuhiro Okada [b,c], Koji Tsumura [e]

[a] Institute of Physics, Meiji Gakuin University, Yokohama 244-8539, Japan
[b] Theory Group, Institute of Particle and Nuclear Studies, KEK, 1-1 Oho, Tsukuba, Ibaraki 305-0801, Japan
[c] Department of Particle and Nuclear Physics, the Graduate University for Advanced Studies (Sokendai), 1-1 Oho, Tsukuba, Ibaraki 305-0801, Japan
[d] Department of Physics, University of Toyama, 3190 Gofuku, Toyama 930-8555, Japan
[e] International Centre for Theoretical Physics, Strada Costiera 11, 34014 Trieste, Italy

ARTICLE INFO

Article history:
Received 31 August 2008
Received in revised form 5 January 2009
Accepted 24 January 2009
Available online 27 January 2009
Editor: T. Yanagida

PACS:
12.60.Fr
14.70.Bh
14.80.Cp

Keywords:
Higgs self-coupling
Photon collider
New physics

ABSTRACT

We calculate the cross section of Higgs boson pair production at a photon collider in the two Higgs doublet model. We focus on the scenario in which the lightest CP even Higgs boson (h) has the Standard Model like couplings to the gauge bosons. We take into account the one-loop correction to the hhh coupling as well as additional one-loop diagrams due to charged Higgs bosons to the $\gamma\gamma \to hh$ helicity amplitudes. It is found that the full cross section can be enhanced by both these effects to a considerable level. We discuss the impact of these corrections on the hhh coupling measurement at the photon collider.

The Higgs sector is the last unknown part of the Standard Model (SM) for elementary particles. Discovery of the Higgs boson and the measurement of its properties at current and future experiments are crucial to establish our basic picture for spontaneous electroweak symmetry breaking (EWSB) and the mechanism of particle mass generation. The Higgs mechanism would be experimentally tested after the discovery of a new scalar particle by measuring its mass and the coupling to the weak gauge bosons. The mass generation mechanism for quarks and charged leptons via the Yukawa interaction is also clarified by the precise determination of both the fermion masses and the Yukawa coupling constants. If the deviation from the SM relation between the mass and the coupling is found, it can be regarded as an evidence of new physics beyond the SM. The nature of EWSB can be revealed through the experimental reconstruction of the Higgs potential, for which the measurement of the Higgs self-coupling is essential [1–5]. The structure of the Higgs potential depends on the scenario of new physics beyond the SM [6,7], so that the experimental determination of the triple Higgs boson coupling can be a probe of each new physics scenario. Furthermore, the property of the Higgs potential would be directly related to the aspect of the electroweak phase transition in the early Universe, which could have impact on the problem of the electroweak baryogenesis [8].

It is known that the measurement of the triple Higgs boson coupling is rather challenging at the CERN Large Hadron Collider (LHC), requiring huge luminosity. A study has shown that at the SLHC with the luminosity of 3000 fb^{-1}, expected accuracy would be about 20–30% for the mass (m_h) of the Higgs boson (h) to be around 170 GeV [1,2]. At the international linear collider (ILC), the main processes for the hhh measurement are the double Higgs boson production mechanisms via the Higgs-strahlung and the W-boson fusion [3,4]. If the collider energy is lower than 1 TeV, the double Higgs strahlung process $e^+e^- \to Zhh$ is important for a light Higgs boson with the mass of 120–140 GeV, while for higher energies the W-boson fusion process $e^+e^- \to hh\nu\bar{\nu}$ becomes dominant due to its t-channel nature [5]. Sensitivity to the hhh coupling in these processes becomes rapidly worse for greater Higgs boson masses. In particular, for the intermediate mass range ($140\ \text{GeV} < m_h < 200\ \text{GeV}$), it has not yet been known how accurately the hhh coupling can be measured by the electron–positron collision.

* Corresponding author.
E-mail addresses: eri@post.kek.jp (E. Asakawa), dharada@post.kek.jp (D. Harada), kanemu@sci.u-toyama.ac.jp (S. Kanemura), yasuhiro.okada@kek.jp (Y. Okada), ktsumura@ictp.it (K. Tsumura).

0370-2693/$ – see front matter
doi:10.1016/j.physletb.2009.01.050

The photon collider is an option of the ILC. The possibility of measuring the hhh coupling via the process of $\gamma\gamma \to hh$ has been discussed in Ref. [9], where the cross section has been calculated at the one-loop level, and the dependence on the triple Higgs boson coupling constant is studied. In Ref. [10] the statistical sensitivity to the hhh coupling constant has been studied especially for a light Higgs boson mass in relatively low energy collisions. Recently, these analyses have been extended for wider regions of the Higgs boson masses and the collider energies. It has been found that when the collision energy is limited to be lower than 500–600 GeV the statistical sensitivity to the hhh coupling can be better for the process in the $\gamma\gamma$ collision than that in the electron–positron collision for the Higgs boson with the mass of 160 GeV [11].

Unlike the double Higgs production processes $e^+e^- \to Zhh$ and $e^+e^- \to hh\nu\bar{\nu}$ in e^+e^- collisions, $\gamma\gamma \to hh$ is an one-loop induced process. When the origin of the shift in the hhh coupling would be due to one-loop corrections by new particles, it may also affect the amplitude of $\gamma\gamma \to hh$ directly through additional one-particle-irreducible (1PI) one-loop diagrams of $\gamma\gamma h$ and $\gamma\gamma hh$ vertices.

In this Letter, we consider the new particle effect on the $\gamma\gamma \to hh$ cross sections in the two Higgs doublet model (THDM), in which additional CP-even, CP-odd and charged Higgs bosons appear. It is known that a non-decoupling one-loop effect due to these extra Higgs bosons can enhance the hhh coupling constant by $\mathcal{O}(100)\%$ [6]. In the $\gamma\gamma \to hh$ helicity amplitudes, there are additional one-loop diagrams by the charged Higgs boson loop to the ordinary SM diagrams (the W-boson loop and the top quark loop). We find that both the charged Higgs boson loop contribution to the $\gamma\gamma \to hh$ amplitudes and the non-decoupling effect on the hhh coupling can enhance the cross section from its SM value significantly. We consider how the new contribution to the cross section of $\gamma\gamma \to hh$ would affect the measurement of the triple Higgs boson coupling at a $\gamma\gamma$ collider.

In order to examine the new physics effect on $\gamma\gamma \to hh$, we calculate the helicity amplitudes in the THDM. We impose a discrete symmetry to the model to avoid flavor changing neutral current in a natural way [12]. The Higgs potential is then given by

$$\begin{aligned} V_{\rm THDM} &= \mu_1^2|\Phi_1|^2 + \mu_2^2|\Phi_2|^2 - \left(\mu_3^2\Phi_1^\dagger\Phi_2 + \text{h.c.}\right) \\ &\quad + \lambda_1|\Phi_1|^4 + \lambda_2|\Phi_2|^4 + \lambda_3|\Phi_1|^2|\Phi_2|^2 \\ &\quad + \lambda_4|\Phi_1^\dagger\Phi_2|^2 + \frac{\lambda_5}{2}\left\{\left(\Phi_1^\dagger\Phi_2\right)^2 + \text{h.c.}\right\}, \end{aligned} \tag{1}$$

where Φ_1 and Φ_2 are two Higgs doublets with hypercharge $+1/2$. We here include the soft breaking term for the discrete symmetry by the parameter μ_3^2. In general, μ_3^2 and λ_5 are complex, but we here take them to be real for simplicity. We parameterize the doublet fields as

$$\Phi_i = \begin{bmatrix} \omega_i^+ \\ \frac{1}{\sqrt{2}}(v_i + h_i + iz_i) \end{bmatrix} \quad (i = 1, 2), \tag{2}$$

where vacuum expectation values (VEVs) v_1 and v_2 satisfy $v_1^2 + v_2^2 = v^2 \simeq (246\ \text{GeV})^2$. The mass matrices can be diagonalized by introducing the mixing angles α and β, where α diagonalizes the mass matrix of the CP-even neutral bosons, and $\tan\beta = v_2/v_1$. Consequently, we have two CP even (h and H), a CP-odd (A) and a pair of charged ($H^\pm$) bosons. We define α such that h is the SM-like Higgs boson when $\sin(\beta - \alpha) = 1$. We do not specify the type of Yukawa interactions [13], because it does not much affect the following discussions.

Throughout this Letter, we concentrate on the case with so-called the SM-like limit [$\sin(\beta - \alpha) = 1$], where the lightest Higgs boson h has the same tree-level couplings as the SM Higgs boson, and the other bosons do not couple to gauge bosons and behave just as extra scalar bosons. In this limit, the masses of the Higgs bosons are[1]

$$m_h^2 = \left\{\lambda_1\cos^4\beta + \lambda_2\sin^4\beta + 2(\lambda_3 + \lambda_4 + \lambda_5)\cos^2\beta\sin^2\beta\right\}v^2, \tag{3}$$

$$m_H^2 = M^2 + \frac{1}{8}\left\{\lambda_1 + \lambda_2 - 2(\lambda_3 + \lambda_4 + \lambda_5)\right\}(1 - \cos 4\beta)v^2, \tag{4}$$

$$m_A^2 = M^2 - \lambda_5 v^2, \tag{5}$$

$$m_{H^\pm}^2 = M^2 - \frac{\lambda_4 + \lambda_5}{2}v^2, \tag{6}$$

where $M(= |\mu_3|/\sqrt{\sin\beta\cos\beta})$ represents the soft breaking scale for the discrete symmetry, and determines the decoupling property of the extra Higgs bosons. When $M \sim 0$, the extra Higgs bosons H, A and $H^\pm$ receive their masses from the VEV, so that the masses are proportional to λ_i. Large masses cause significant non-decoupling effect in the radiative correction to the hhh coupling. On the other hand, when $M \gg v$ the masses are determined by M. In this case, the quantum effect decouples for $M \to \infty$.

There are several important constraints on the THDM parameters from the data. The LEP direct search results give the lower bounds $m_h > 114$ GeV in the SM-like limit and m_H, m_A, $m_{H^\pm} \gtrsim$ 80–90 GeV [14]. In addition, the rho parameter data at the LEP requires the approximate custodial symmetry in the Higgs potential. This implies that $m_{H^\pm} \simeq m_A$ or $\sin(\beta - \alpha) \simeq 1$ and $m_{H^\pm} \simeq m_H$. The Higgs potential is also constrained from the tree level unitarity [15,16], the triviality and the vacuum stability [17], in particular for the case where the non-decoupling effect is important as in the discussion here. For $M \sim 0$, masses of the extra Higgs bosons H, A and $H^\pm$ are bounded from above by about 500 GeV for $\tan\beta = 1$, when they are degenerated [15]. With non-zero M, these bounds are relaxed depending on the value of M. The constraint from $b \to s\gamma$ gives a lower bound on the mass of $H^\pm$ depending on the type of Yukawa interaction; i.e., in Model II [13], $m_{H^\pm} > 295$ GeV (95% CL) [18]. Recent data for $B \to \tau\nu$ can also give a constraint on the charged Higgs mass especially for large values of $\tan\beta$ in Model II [19,20]. In the following analysis, we do not include these constraints from B-physics because we do not specify type of Yukawa interactions.

In the THDM with $\sin(\beta - \alpha) = 1$, the one-loop helicity amplitudes for the initial photon helicities ℓ_1 and ℓ_2 ($\ell_i = +1$ or -1) are given as

$$\mathcal{M}_{\rm THDM}^{\text{1-loop}}(\ell_1, \ell_2) = \mathcal{M}(\ell_1, \ell_2, \lambda_{hhh}) + \Delta\mathcal{M}(\ell_1, \ell_2, \lambda_{hhh}), \tag{7}$$

where $\lambda_{hhh} = -3m_h^2/v$, $\mathcal{M}(\ell_1, \ell_2, \lambda_{hhh})$ is the SM amplitude given in Ref. [9], and $\Delta\mathcal{M}(\ell_1, \ell_2, \lambda_{hhh})$ represents additional one-loop contributions from the charged Higgs boson loop to the $\gamma\gamma \to hh$ cross section. We note that λ_{hhh} has the same form as in the SM when $\sin(\beta - \alpha) = 1$. Due to the parity we have $\mathcal{M}_{\rm THDM}(\ell_1, \ell_2) = \mathcal{M}_{\rm THDM}(-\ell_1, -\ell_2)$, so that there are independent two helicity amplitudes.

The Feynman diagrams which contribute to $\Delta\mathcal{M}$ are shown in Fig. 1. $\Delta\mathcal{M}$ is given for each helicity set for $\sin(\beta - \alpha) \simeq 1$ as

[1] For the case without the SM-like limit, see Ref. [7] for example.

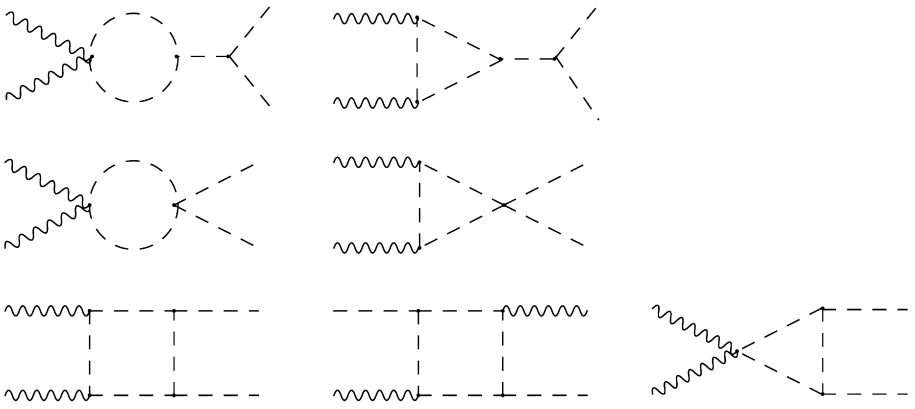

Fig. 1. Feynman diagrams for charged Higgs boson contributions to $\gamma\gamma \to hh$. Wavy lines represent photons, dotted lines in loops represent charged Higgs bosons $H^\pm$, and other dotted lines are the neutral Higgs bosons.

$$
\begin{aligned}
&\alpha_W \Delta\mathcal{M}(+,+,\lambda_{hhh}) \\
&= \frac{12\lambda_{hH^+H^-}\lambda_{hhh}}{\hat{s}-m_h^2}\left\{C_{24}(\hat{s}) - \frac{1}{4}B_0(\hat{s}, m_{H^\pm}, m_{H^\pm})\right\} \\
&\quad + 4\lambda_{hhH^+H^-}B_0(\hat{s}, m_{H^\pm}, m_{H^\pm}) - (\lambda_{hH^+H^-})^2\tilde{C}_0(\hat{s}) \\
&\quad - 4\lambda_{hhH^+H^-}C_{24}(\hat{s}) \\
&\quad + (\lambda_{hH^+H^-})^2\left\{\left(D_{27}^{1234} + D_{27}^{1243} + D_{27}^{2134} + D_{27}^{2143}\right)\right. \\
&\quad \left. - \frac{1}{2\hat{s}}\left(\hat{t}\hat{u} - m_h^4\right)\left(D_{23}^{1234} + D_{23}^{1243} + D_{23}^{2134} + D_{23}^{2143}\right)\right\}, \qquad (8)
\end{aligned}
$$

and

$$
\begin{aligned}
&\alpha_W \Delta\mathcal{M}(+,-,\lambda_{hhh}) \\
&= -(\lambda_{hH^+H^-})^2\frac{1}{2\hat{s}}\left(\hat{t}\hat{u} - m_h^4\right)\left(D_{23}^{1234} + D_{23}^{1243} + D_{23}^{2134} + D_{23}^{2143}\right), \qquad (9)
\end{aligned}
$$

where $\hat{s}$, $\hat{t}$ and $\hat{u}$ are ordinary Mandelstam variables for the sub processes, and $C_{24}(\hat{s}) = C_{24}(0,0,\hat{s}, m_{H^\pm}, m_{H^\pm}, m_{H^\pm})$, $\tilde{C}_0(\hat{s}) = C_0(m_h^2, m_h^2, \hat{s}, m_{H^\pm}, m_{H^\pm}, m_{H^\pm})$, and $D_{ab}^{ijkl} = D_{ab}(p_i^2, p_j^2, p_k^2, p_l^2, m_{H^\pm}, m_{H^\pm}, m_{H^\pm}, m_{H^\pm})$. Here we employ the Passarino–Veltman formalism in Ref. [21]. We take the same normalization for these amplitudes as in Ref. [9]. We note that $\Delta\mathcal{M}(+,-,\lambda_{hhh})$ is independent of λ_{hhh} because of no $\hat{s}$-channel diagram contribution. The scalar coupling constants $\lambda_{hH^+H^-}$ and $\lambda_{hhH^+H^-}$ are defined by

$$
\lambda_{hH^+H^-} = 2\lambda_{hhH^+H^-} = -\left(\frac{m_h^2}{v} + 2\frac{m_{H^\pm}^2 - M^2}{v}\right). \qquad (10)
$$

The relative sign between $\mathcal{M}(\ell_1,\ell_2,\lambda_{hhh})$ and $\Delta\mathcal{M}(\ell_1,\ell_2,\lambda_{hhh})$ has been checked to be consistent with the results for the effective Lagrangian in Eq. (19) in Ref. [22] in the large mass limit for inner particles.

In Eq. (7), λ_{hhh} is the tree level coupling constant. It is known that in the THDM λ_{hhh} can be changed by the one-loop contribution of extra Higgs bosons due to the non-decoupling effect (when $M \sim 0$). In the following analysis, we include such an effect on the cross sections replacing λ_{hhh} by the effective coupling $\Gamma_{hhh}^{\rm THDM}(\hat{s}, m_h^2, m_h^2)$, which is evaluated at the one-loop level as [6]

$$
\begin{aligned}
&\Gamma_{hhh}^{\rm THDM}\left(\hat{s}, m_h^2, m_h^2\right) \\
&\simeq -\frac{3m_h^2}{v}\left[1 + \sum_{\Phi=H,A,H^+,H^-}\frac{m_\Phi^4}{12\pi^2 v^2 m_h^2}\left(1 - \frac{M^2}{m_\Phi^2}\right)^3\right. \\
&\quad \left. - \frac{N_c m_t^4}{3\pi^2 v^2 m_h^2}\right]. \qquad (11)
\end{aligned}
$$

As a striking feature, there are quartic power contributions of the masses of extra Higgs bosons which are divided by $v^2 m_h^2$, when $M \sim 0$. Thus, the large mass of the extra Higgs boson (H, A, $H^\pm$) with the lighter SM-like Higgs boson h would cause large quantum corrections to the hhh coupling, which amount to 50–100%. This effect can be regarded as the leading two loop contribution to $\gamma\gamma \to hh$ in our analysis. The exact one-loop formula for $\Gamma_{hhh}^{\rm THDM}$ is given in Ref. [7], which has been used in our actual numerical analysis.

Finally, the cross section for the each subprocess is given by[2]

$$
\frac{d\hat{\sigma}(\ell_1,\ell_2)}{d\hat{t}} = \frac{\alpha^2\alpha_W^2}{32\pi\hat{s}^2}\left|\mathcal{M}_{\rm THDM}(\ell_1,\ell_2)\right|^2, \qquad (12)
$$

where $\mathcal{M}_{\rm THDM}^{\text{2-loop}}(\ell_1,\ell_2)$ is defined by

$$
\mathcal{M}_{\rm THDM}^{\text{2-loop}}(\ell_1,\ell_2) = \mathcal{M}\left(\ell_1,\ell_2,\Gamma_{hhh}^{\rm THDM}\right) + \Delta\mathcal{M}\left(\ell_1,\ell_2,\Gamma_{hhh}^{\rm THDM}\right). \qquad (13)
$$

We comment on the consistency of our perturbation calculation. One might think that the inclusion of the one-loop corrected hhh vertex function $\Gamma_{hhh}^{\rm THDM}$ in the calculation of the cross section $\gamma\gamma \to hh$ would be inconsistent unless we also take all the other two loop contributions into account. Our calculation can be justified in the following sense. First of all, $\Gamma_{hhh}^{\rm THDM}$ is a gauge invariant subset. Second, it can be seen from Eq. (11) that the deviation from the SM value $\Delta\Gamma_{hhh}^{\rm THDM}/\Gamma_{hhh}^{\rm SM}$ ($\equiv \Gamma_{hhh}^{\rm THDM}/\Gamma_{hhh}^{\rm SM} - 1$), where $\Gamma_{hhh}^{\rm SM}$ is one-loop vertex function of hhh in the SM given in Ref. [7], can be of $\mathcal{O}(1)$ for the case of M^2, $m_h^2 \ll m_\Phi^2$, whereas the contributions from the other two loop diagrams do not contain the factor m_Φ^2/m_h^2, and thus relatively unimportant for $m_\Phi^2 \gg m_h^2$. Therefore, we can safely neglect these effects as compared to the non-decoupling loop effect in the hhh coupling. The details are shown in Appendix A.

In Fig. 2, the cross sections of $\gamma\gamma \to hh$ for the helicity set $(+,+)$ are shown as a function of the photon–photon collision energy $E_{\gamma\gamma}$. In the left [right] figure, parameters are chosen to be $m_h = 120$ GeV [$m_h = 160$ GeV], $\sin(\beta-\alpha) = 1$, $\tan\beta = 1$, $M = 0$ and $m_H = m_A = m_{H^\pm} = 400$ GeV. In this case, $\Delta\Gamma_{hhh}^{\rm THDM}/\Gamma_{hhh}^{\rm SM}$ amounts to about 120% for $m_h = 120$ GeV (80% for $m_h = 160$ GeV) [6].[3] The five curves in each figure correspond to the following cases:

(a) THDM 2-loop: the cross section in the THDM with additional one-loop corrections to the hhh vertex, $\Gamma_{hhh}^{\rm THDM}$; i.e., the contribution from $\mathcal{M}_{\rm THDM}^{\text{2-loop}}(+,+)$ in Eq. (13).

[2] The right-hand side of Eq. (12) is different from the formula in Ref. [9] by factor 1/2, but Eq. (12) reproduces figures shown in Ref. [9].

[3] The results of $\Delta\Gamma_{hhh}^{\rm THDM}/\Gamma_{hhh}^{\rm SM}$ with $M \neq 0$ are given in Ref. [6].

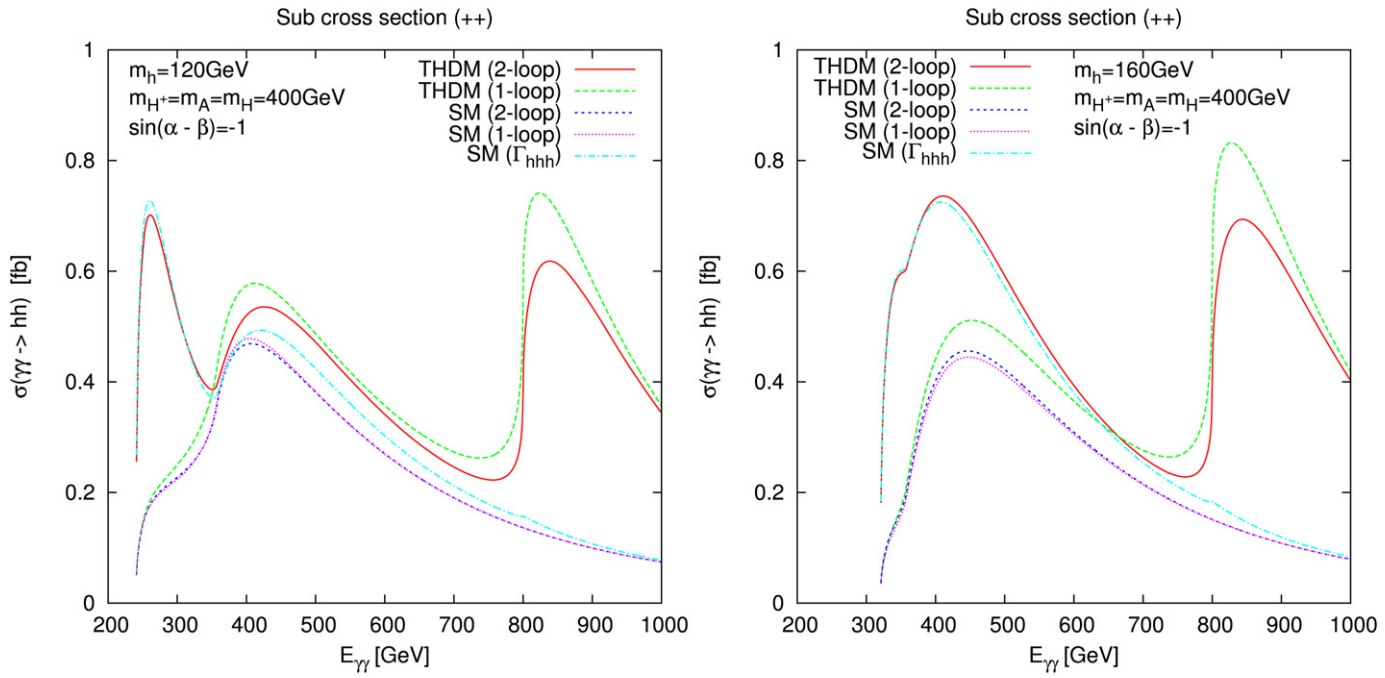

Fig. 2. The cross section $\hat{\sigma}(+,+)$ for the sub process $\gamma\gamma \to hh$ with the photon helicity set $(+,+)$ as a function of the collision energy $E_{\gamma\gamma}$. In the left [right] figure the parameters are taken to be $m_h = 120$ [160] GeV for $m_\Phi (\equiv m_H = m_A = m_{H^\pm}) = 400$ GeV, $\sin(\beta-\alpha) = 1$, $\tan\beta = 1$ and $M = 0$.

(b) THDM 1-loop: the cross section in the THDM with the tree level *hhh* coupling constant λ_{hhh}; i.e., the contribution from $\mathcal{M}^{\text{1-loop}}_{\text{THDM}}(+,+)$ in Eq. (7).
(c) SM 2-loop: the cross section in the SM with additional top loop correction to the *hhh* coupling Γ^{SM}_{hhh} given in Ref. [7].
(d) SM 1-loop: the cross section in the SM with the tree level *hhh* coupling constant $\lambda^{\text{SM}}_{hhh}$ $(= \lambda_{hhh}$ for $\sin(\beta-\alpha) = 1)$.
(e) For comparison, we also show the result which corresponds to the SM 1-loop result with the effective *hhh* coupling $\Gamma^{\text{THDM}}_{hhh}$.

In the left figure, there are three peaks in the 2-loop THDM cross section. The one at the lowest $E_{\gamma\gamma}$ is the peak just above the threshold of *hh* production. There the cross section is by about factor three enhanced as compared to the SM prediction due to the effect of $\Delta\Gamma^{\text{THDM}}_{hhh}/\Gamma^{\text{SM}}_{hhh}$ $(\sim 120\%)$ because of the dominance of the pole diagrams in $\gamma\gamma \to hh$. The second peak at around $E_{\gamma\gamma} \sim 400$ GeV comes from the top quark loop contribution which is enhanced by the threshold of top pair production. Around this point, the 2-loop THDM cross section in the case (a) can be well described by that in the case (e). For $E_{\gamma\gamma} \sim 400$–$600$ GeV, the cross section in the THDM 2-loop result deviates from the SM value due to both the charged Higgs loop effect in $\Delta\mathcal{M}$ and the effect of $\Delta\Gamma^{\text{THDM}}_{hhh}/\Gamma^{\text{SM}}_{hhh}$. The third peak at around $E_{\gamma\gamma} \sim 850$ GeV is the threshold enhancement of the charged Higgs boson loop in $\Delta\mathcal{M}$, where the real production of charged Higgs bosons occurs. The contribution from the non-pole one-loop diagrams is dominant. In the right figure, we can see two peaks around $E_{\gamma\gamma} \sim$ 350–400 GeV and 850 GeV. At the first peak, the contribution from the pole diagrams is dominant so that the cross section is largely enhanced by the effect of $\Delta\Gamma^{\text{THDM}}_{hhh}/\Gamma^{\text{SM}}_{hhh}$ by several times 100% for $E_{\gamma\gamma} \sim 350$ GeV. It also amounts to about 80% for $E_{\gamma\gamma} \sim 400$ GeV. For $E_{\gamma\gamma} < 600$–700 GeV, the result in the case (e) gives a good description of that in the case (a). The second peak is due to the threshold effect of the real H^+H^- production as in the left figure.

The full cross section of $e^-e^- \to \gamma\gamma \to hh$ is given from the sub cross sections by convoluting the photon luminosity spectrum [9]:

$$d\sigma = \int_{4m_h^2/s}^{y_m^2} d\tau \frac{dL_{\gamma\gamma}}{d\tau}\left\{\frac{1+\xi_1\xi_2}{2}d\hat{\sigma}(+,+) + \frac{1-\xi_1\xi_2}{2}d\hat{\sigma}(+,-)\right\}, \quad (14)$$

where $\sqrt{s}$ is the centre-of-mass energy of the e^-e^- system, and

$$\frac{dL_{\gamma\gamma}}{d\tau} = \int_{\tau/y_m}^{y_m} \frac{dy}{y} f_\gamma(x,y) f_\gamma(x,\tau/y), \quad (15)$$

where $\tau = \hat{s}/s$, $y = E_\gamma/E_b$ with E_γ and E_b being the energy of photon and electron beams respectively, and $y_m = x/(1+x)$ with $x = 4E_b\omega_0/m_e^2$ where ω_0 is the laser photon energy and m_e is the electron mass. In our study, we set $x = 4.8$. The photon momentum distribution function $f_\gamma(x,y)$ and mean helicities of the two photon beams ξ_i $(i = 1,2)$ are given in Ref. [23].

In Fig. 3, the full cross sections of $e^-e^- \to \gamma\gamma \to hh$ are shown for $m_h = 120$ GeV in the left figure and $m_h = 160$ GeV in the right figure, respectively, as a function of $\sqrt{s}$ for various values of the extra Higgs boson masses m_Φ $(\equiv m_H = m_A = m_{H^\pm})$ in the cases of $\tan\beta = 1$, $\sin(\beta-\alpha) = 1$ and $M = 0$. In order to extract the contribution from $\hat{\sigma}(+,+)$ that is sensitive to the *hhh* vertex, we take the polarizations of the initial laser beam to be both -1, and those for the initial electrons to be both $+0.45$ [9]. The full cross section for $m_\Phi = 400$ GeV has similar energy dependences to the sub cross section $\hat{\sigma}(+,+)$ in Fig. 2, where corresponding energies are rescaled approximately by around $\sqrt{s} \sim E_{\gamma\gamma}/0.8$ due to the photon luminosity spectrum. For smaller m_Φ, the peak around $\sqrt{s} \sim 350$ GeV becomes lower because of smaller $\Delta\Gamma^{\text{THDM}}_{hhh}/\Gamma^{\text{SM}}_{hhh}$.

In Fig. 4, the full cross sections are shown as a function of m_Φ for $m_h = 120$ GeV at $\sqrt{s} = 350$ GeV (the left figure) and $m_h = 160$ GeV at $\sqrt{s} = 600$ GeV (the right figure). In each figure, five curves correspond to the cases (a)–(e) in Fig. 2. The other parameters are taken to be $\sin(\beta-\alpha) = 1$, $\tan\beta = 1$ and $M = 0$. In the left figure, one can see that the cross section is enhanced due to the enlarged $\Gamma^{\text{THDM}}_{hhh}$ for larger values of m_Φ which is proportional to m_Φ^4 (when $M \sim 0$). This implies that the cross section

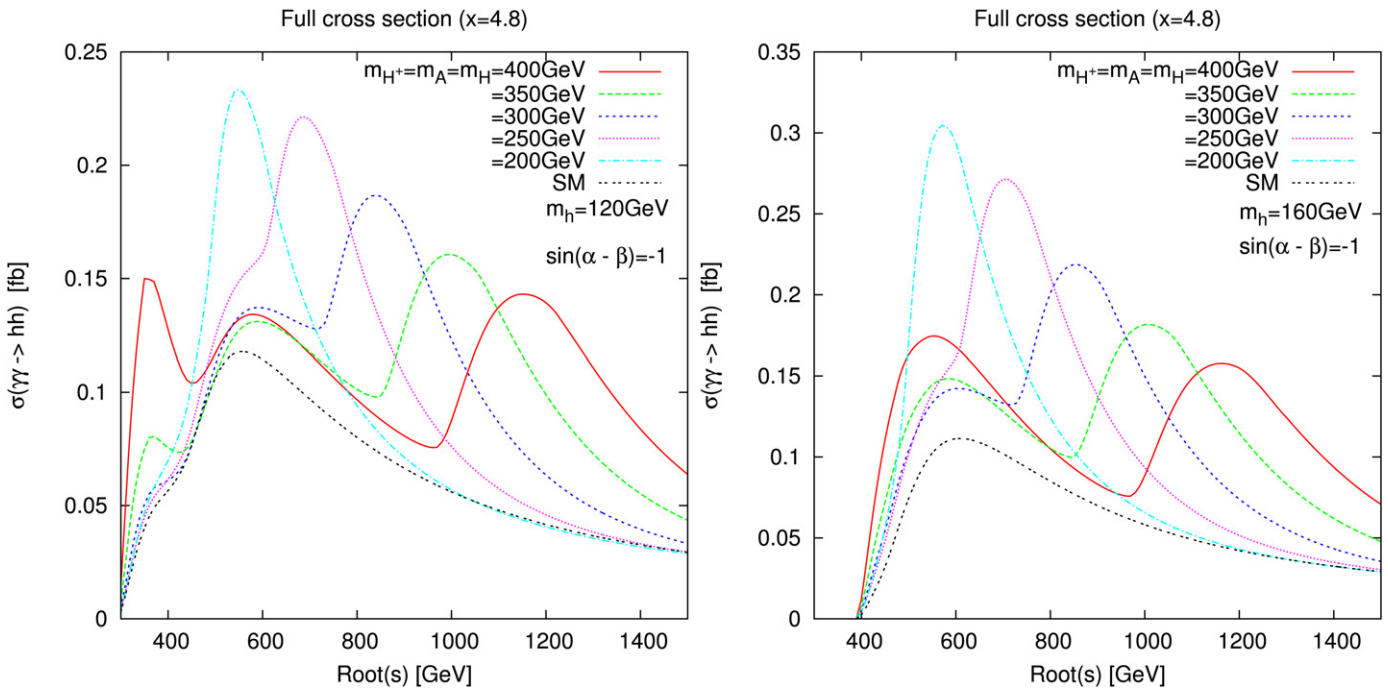

Fig. 3. The full cross section of $e^-e^- \to \gamma\gamma \to hh$ as a function of $\sqrt{s}$ for each value of $m_\Phi (= m_H = m_A = m_{H^\pm})$ with $\sin(\beta-\alpha)=1$, $\tan\beta = 1$ and $M = 0$. The case for $m_h = 120$ [160] GeV is shown in the left [right] figure.

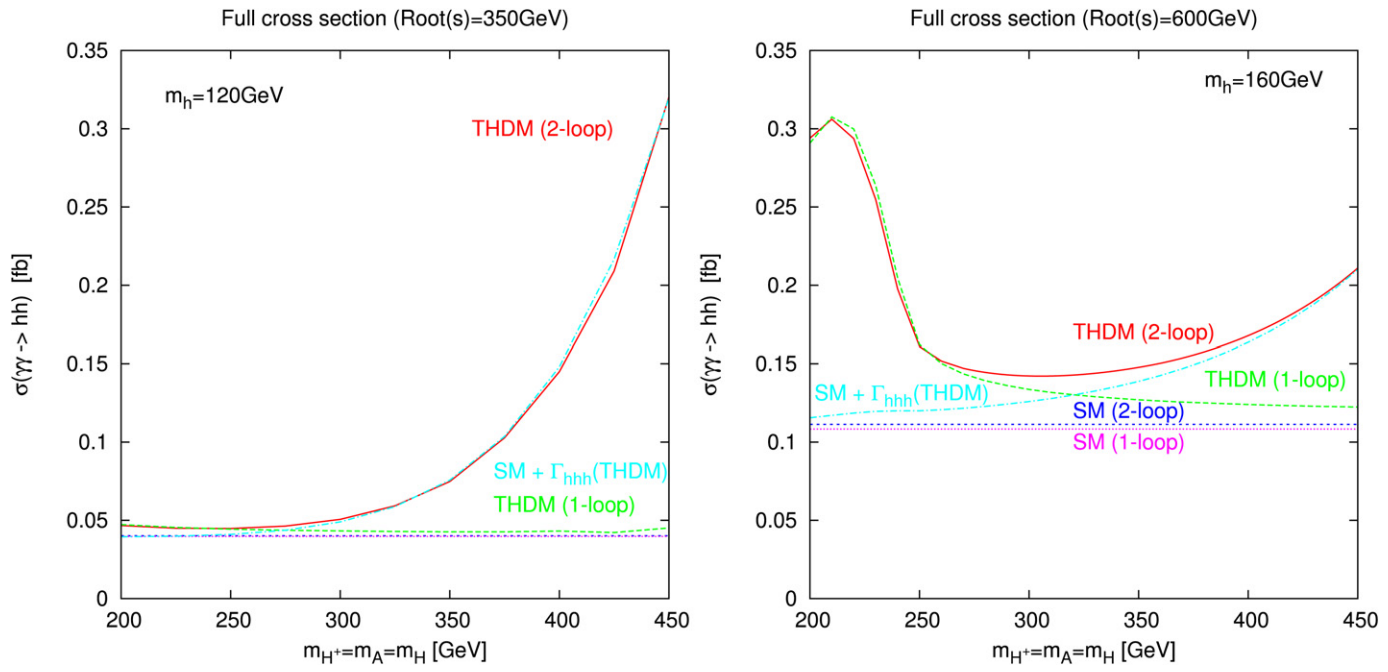

Fig. 4. In the left [right] figure, the full cross section of $e^-e^- \to \gamma\gamma \to hh$ at $\sqrt{s} = 350$ GeV [600 GeV] for $m_h = 120$ [160] GeV is shown as a function of $m_\Phi (= m_H = m_A = m_{H^\pm})$ with $\sin(\beta-\alpha)=1$, $\tan\beta = 1$ and $M = 0$.

for these parameters is essentially determined by the pole diagram contributions. The effect of the charged Higgs boson loop from $\Delta\mathcal{M}$ is relatively small since the threshold of charged Higgs boson production is far. Therefore, the deviation in the cross section from the SM value is smaller for relatively small m_Φ (10–20% for $m_\Phi < 300$ GeV due to the charged Higgs loop effect in $\Delta\mathcal{M}$) but it becomes rapidly enhanced for greater values of m_Φ ($\mathcal{O}(100)$% for $m_\Phi > 350$ GeV due to the large $\Delta\Gamma_{hhh}^{\rm THDM}$). A similar enhancement for the large m_Φ values can be seen in the right figure. The enhancement in the cross section in the THDM can also be seen for $m_\Phi < 250$ GeV, where the threshold effect of the charged Higgs boson loop in $\Delta\mathcal{M}$ appears around $\sqrt{s} \sim 600$ GeV in addition to that of the top quark loop diagrams in $\mathcal{M}$. For $m_\Phi = 250$–400 GeV, both contributions from the charged Higgs boson loop contribution and the effective hhh coupling are important and enhance the cross section from its SM value by 40–50%.

We have analysed the new physics loop effects on the cross section of $\gamma\gamma \to hh$ in the THDM including the next to leading effect due to the extra Higgs boson loop diagram in the hhh vertex. Our analysis shows that the cross section can be largely changed from the SM prediction by the two kinds of contributions; i.e., additional contribution by the charged Higgs boson loop

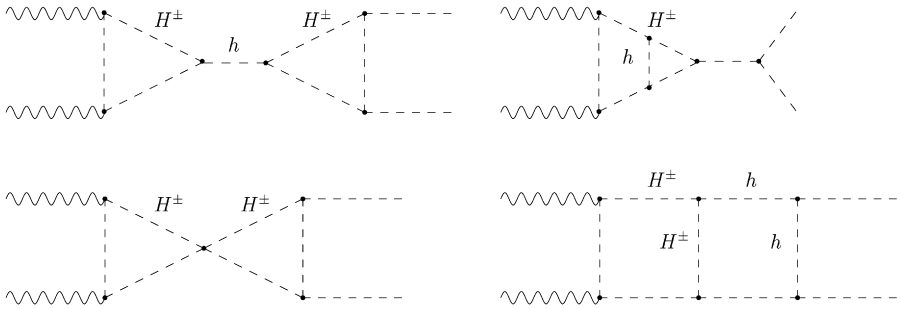

Fig. 5. Example of the two-loop diagrams contributing to $\gamma\gamma \to hh$.

in $\Delta\mathcal{M}$, and the effective one-loop hhh vertex $\Gamma^{\rm THDM}_{hhh}$ enhanced by the non-decoupling effect of extra Higgs bosons. The cross section strongly depends on m_h and $\sqrt{s}$ and also on m_Φ. The approximation of the full cross section in the case (a) (2-loop THDM) by using the result in the case (e) (SM + $\Gamma^{\rm THDM}_{hhh}$) is a good description for $\sqrt{s} \ll 2m_\Phi/0.8$. On the other hand, in a wide region between threshold of top pair production and that of charged Higgs boson pair production, both the contributions (those from $\Delta\mathcal{M}$ and from $\Gamma^{\rm THDM}_{hhh}$) are important. In the region below the threshold of the real production of extra Higgs bosons, the cross section can be a few times 0.1 fb in the THDM while that in the SM is about 0.05 fb. Such differences from the SM prediction would be detectable at a future photon collider.

We note that the analysis in this Letter can be applied to the models [24] in which extra charged scalar bosons appear with a potentially large loop correction in the hhh coupling.

Note added

After this work was finished, we noticed the paper [25] which studied $\gamma\gamma \to hh$ in the THDM. Our Letter includes the additional contribution of the hhh vertex (the leading two-loop effect on $\gamma\gamma \to hh$), which was not considered in [25].

Acknowledgements

The work of S.K. was supported in part by Grant-in-Aid for Science Research, Japan Society for the Promotion of Science (JSPS), No. 18034004. The work of Y. O. was supported in part by Grant-in-Aid for Science Research, MEXT-Japan, No. 16081211, and JSPS, No. 20244037.

Appendix A

If the mass of the particle in the loop comes from the VEV, a large mass implies a large coupling constant, so that a naive argument of the decoupling theorem is not applied. It is known that in such a case a powerlike mass contribution of particles in the loop appears in the one-loop contribution. This is called the non-decoupling effect.

When one-loop corrected hhh vertex $\Gamma^{\rm THDM}_{hhh}$ largely deviates from $\Gamma^{\rm SM}_{hhh}$ due to the non-decoupling property of the extra Higgs bosons, the main two loop contribution to $\gamma\gamma \to hh$ comes from the s-channel diagrams with the effective hhh coupling. We here show this by the use of a power counting method. For simplicity, we consider the leading powerlike effect of the mass of particles in the loops in the two-loop diagrams for the case with $M \sim 0$ where masses of extra Higgs bosons are proportional to the VEV so that the non-decoupling effect is maximal.

When $M \sim 0$, the coupling constants of hH^+H^- and hhH^+H^- are proportional to $m^2_{H^\pm}/v$ and $m^2_{H^\pm}/v^2$, respectively. We consider the situation that $m_{H^\pm} \gg \sqrt{s} > 2m_h$. The leading non-decoupling effect of the $H^\pm$ one-loop triangle-type diagram in Fig. 1(up-right) and that of the $H^\pm$ one-loop box-type diagram in Fig. 1(bottom-left) are evaluated as

$$\mathcal{M}^{\text{1-loop}}_{\rm trig} \propto \frac{1}{16\pi^2}\frac{q^2}{v}\frac{1}{s-m_h^2}\left(\frac{m_h^2}{v}\right) \sim \frac{q^2}{(4\pi v)^2}, \tag{A.16}$$

$$\mathcal{M}^{\text{1-loop}}_{\rm box} \propto \frac{1}{16\pi^2}\frac{q^2}{v^2} \sim \frac{q^2}{(4\pi v)^2}, \tag{A.17}$$

where we used the fact that the effective $\gamma\gamma h$ and $\gamma\gamma hh$ vertices come from the dimension six operator $|\Phi_i|^2 F_{\mu\nu}F^{\mu\nu}$, so that they are proportional to q^2/v and q^2/v^2 at the leading order, respectively, where $q^2 \sim s$. Therefore, the effect of $m_{H^\pm}$ on $\gamma\gamma \to hh$ can be at most $\log m_{H^\pm}$ at the one-loop level. A similar conclusion of power counting can also be obtained for one-loop effects of top and bottom quarks and W bosons to $\gamma\gamma \to hh$.

Next, let us examine two-loop diagrams shown in Fig. 5. The non-decoupling effect in the diagram (a) in Fig. 5(up-left) is calculated as

$$\begin{aligned}\mathcal{M}^{\text{2-loop}}_{\rm (a)} &\propto \left(\frac{1}{16\pi^2}\right)^2\frac{q^2}{v}\frac{1}{s-m_h^2}\left(\frac{m^2_{H^\pm}}{v}\right)^3\frac{d^4k}{(k^2-m^2_{H^\pm})^3}\\ &\sim \frac{q^2}{(4\pi v)^2}\left(\frac{m^4_{H^\pm}}{(4\pi v)^2 m_h^2}\right),\end{aligned} \tag{A.18}$$

where momenta of external lines are neglected, and k is the momentum in the loop of the effective hhh vertex, which is replaced by the greatest dimensionful parameter of the system; i.e. $m_{H^\pm}$. This result of the power counting is not changed even after the renormalization of the hhh vertex is performed [6]. There are other two loop diagrams which are generated from the s-channel type one-loop diagram, such as the diagram (b) in Fig. 5(up-right) where there is the bridge of h in the $H^\pm$ triangle type loop. Its non-decoupling effect is evaluated as

$$\begin{aligned}\mathcal{M}^{\text{2-loop}}_{\rm (b)} &\propto \left(\frac{1}{16\pi^2}\right)^2\frac{q^2}{v}\left(\frac{m^2_{H^\pm}}{v}\right)^2\frac{d^4k}{(k^2-m^2_{H^\pm})^3}\frac{1}{s-m_h^2}\left(\frac{m_h^2}{v}\right)^2\\ &\sim \frac{q^2}{(4\pi v)^2}\left(\frac{m^2_{H^\pm}}{(4\pi v)^2}\right).\end{aligned} \tag{A.19}$$

The dependence on $m_{m^\pm_H}$ is not quartic but quadratic. We have examined all the other two-loop diagrams which are generated from the one-loop s-channel diagram and confirmed that they are the same or less power dependence on $m^\pm_H$ as the diagram (b).

A similar counting can also be applied for the diagrams such as the diagram (c) in Fig. 5(down-left) where charged Higgs bosons are running in the both loops, and the diagram (d) in Fig. 5(down-right) where ladder of h is added to the one-loop box type diagram;

$$\mathcal{M}^{\text{2-loop}}_{\text{(c)}} \propto \left(\frac{1}{16\pi^2}\right)^2 \frac{q^2}{v^2} \frac{d^4k}{(k^2-m_{H^\pm}^2)^3} \left(\frac{m_{H^\pm}^2}{v}\right)^2 \sim \frac{q^2}{(4\pi v)^2}\left(\frac{m_{H^\pm}^2}{(4\pi v)^2}\right), \tag{A.20}$$

$$M^{\text{2-loop}}_{\text{(d)}} \propto \left(\frac{1}{16\pi^2}\right)^2 \frac{q^2}{v^2} \frac{d^4k}{(k^2-m_h^2)^3} \left(\frac{m_h^2}{v}\right)^2 \sim \frac{q^2}{(4\pi v)^2}\left(\frac{m_h^4}{(4\pi v)^2 m_{H^\pm}^2}\right). \tag{A.21}$$

We find that all the 1PI two-loop diagrams of $\gamma\gamma hh$ also have the quadratic or less power dependences on $m_{H^\pm}$.

The power dependence on $m_{H^\pm}$ in the two point function of h can be reduced by the renormalization of mass m_h^2, but the highest power of $m_{H^\pm}$ in the 1PI two loop diagrams of $\gamma\gamma hh$ does not change by the renormalization.

In conclusion, the non-decoupling effect of $H^\pm$ on the renormalized amplitude of $\gamma\gamma \to hh$ at the two loop level can be described as

$$\mathcal{M}^{\text{2-loop}} \propto \frac{q^2}{(4\pi v)^2}\left[1 + \mathcal{O}\left(\frac{m_{H^\pm}^4}{(4\pi v)^2 m_h^2}\right) + \mathcal{O}\left(\frac{m_{H^\pm}^2}{(4\pi v)^2}\right)\right], \tag{A.22}$$

where the second term in the right-hand side comes from the s-channel diagrams which include the one-loop corrected hhh vertex. For the case where non-decoupling property of the extra Higgs bosons is important, the contribution from this term is dominant when $m_{H^\pm} \gg m_h$. Although we gave the explanation for the charged Higgs loop effects, this argument can also be applied to loop effects of all quarks, gauge bosons and extra Higgs bosons with non-decoupling property.

References

[1] U. Baur, T. Plehn, D.L. Rainwater, Phys. Rev. Lett. 89 (2002) 151801, hep-ph/0206024;
U. Baur, T. Plehn, D.L. Rainwater, Phys. Rev. D 67 (2003) 033003, hep-ph/0211224.

[2] U. Baur, T. Plehn, D.L. Rainwater, Phys. Rev. D 68 (2003) 033001, hep-ph/0304015.

[3] G. Gounaris, D. Schildknecht, F.M. Renard, Phys. Lett. B 83 (1979) 191;
V. Barger, et al., Phys. Rev. D 49 (1994) 79;
A. Djouadi, H.E. Haber, P.M. Zerwas, Phys. Lett. B 375 (1996) 203, hep-ph/9602234;
V.A. Ilyn, et al., Phys. Rev. D 54 (1996) 6717.

[4] W. Kilian, M. Kramer, P.M. Zerwas, Phys. Lett. B 373 (1996) 135, hep-ph/9512355;
J.i. Kamoshita, Y. Okada, M. Tanaka, I. Watanabe, hep-ph/9602224;
A. Djouadi, W. Kilian, M. Muhlleitner, P.M. Zerwas, Eur. Phys. J. C 10 (1999) 45, hep-ph/9904287;
G. Belanger, et al., Phys. Lett. B 576 (2003) 152, hep-ph/0309010.

[5] C. Castanier, P. Gay, P. Lutz, J. Orloff, hep-ex/0101028;
M. Battaglia, E. Boos, W.-M. Yao, hep-ph/0111276;
Y. Yasui, et al., hep-ph/0211047;
Talk given by S. Yamashita at LCWS2004, http://polywww.in2p3.fr/actualites/congres/lcws2004/.

[6] S. Kanemura, S. Kiyoura, Y. Okada, E. Senaha, C.P. Yuan, Phys. Lett. B 558 (2003) 157, hep-ph/0211308.

[7] S. Kanemura, Y. Okada, E. Senaha, C.P. Yuan, Phys. Rev. D 70 (2004) 115002, hep-ph/0408364.

[8] C. Grojean, G. Servant, J.D. Wells, Phys. Rev. D 71 (2005) 036001, hep-ph/0407019;
S. Kanemura, Y. Okada, E. Senaha, Phys. Lett. B 606 (2005) 361, hep-ph/0411354;
S.W. Ham, S.K. Oh, hep-ph/0502116.

[9] G.V. Jikia, Nucl. Phys. B 412 (1994) 57.

[10] R. Belusevic, G. Jikia, Phys. Rev. D 70 (2004) 073017, hep-ph/0403303.

[11] E. Asakawa, D. Harada, S. Kanemura, Y. Okada, K. Tsumura, talk given by E. Asakawa at LEI 2007 (http://home.hiroshima-u.ac.jp/lei2007/index.html), and talk given by S. Kanemura at TILC 08 (http://www.awa.tohoku.ac.jp/TILC08/).

[12] S.L. Glashow, S. Weinberg, Phys. Rev. D 15 (1977) 1958.

[13] V.D. Barger, J.L. Hewett, R.J.N. Phillips, Phys. Rev. D 41 (1990) 3421.

[14] C. Amsler, et al., Particle Data Group, Phys. Lett. B 667 (2008) 1.

[15] S. Kanemura, T. Kubota, E. Takasugi, Phys. Lett. B 313 (1993) 155.

[16] H. Huffel, G. Pocsik, Z. Phys. C 8 (1981) 13;
J. Maalampi, J. Sirkka, I. Vilja, Phys. Lett. B 265 (1991) 371;
A.G. Akeroyd, A. Arhrib, E.M. Naimi, Phys. Lett. B 490 (2000) 119, hep-ph/0006035;
I.F. Ginzburg, I.P. Ivanov, Phys. Rev. D 72 (2005) 115010, hep-ph/0508020.

[17] S. Nie, M. Sher, Phys. Lett. B 449 (1999) 89, hep-ph/9811234;
S. Kanemura, T. Kasai, Y. Okada, Phys. Lett. B 471 (1999) 182, hep-ph/9903289.

[18] M. Ciuchini, G. Degrassi, P. Gambini, G.F. Giudice, Nucl. Phys. B 527 (1998) 21;
P. Ciafaloni, A. Romanino, A. Strumia, Nucl. Phys. B 524 (1998) 361;
F. Borzumati, G. Greub, Phys. Rev. D 58 (1998) 074004;
T.M. Aliev, E.O. Iltan, Phys. Rev. D 58 (1998) 095014;
M. Misiak, et al., Phys. Rev. Lett. 98 (2007) 022002, hep-ph/0609232.

[19] K. Ikado, et al., Belle Collaboration, Phys. Rev. Lett. 97 (2006) 251802, hep-ex/0604018;
B. Aubert, et al., BaBar Collaboration, hep-ex/0608019.

[20] M. Krawczyk, D. Sokolowska, arXiv: 0711.4900 [hep-ph].

[21] G. Passarino, M.J.G. Veltman, Nucl. Phys. B 160 (1979) 151.

[22] A.I. Vainshtein, M.B. Voloshin, V.I. Zakharov, M.A. Shifman, Sov. J. Nucl. Phys. 30 (5) (1979).

[23] I.F. Ginzburg, G.L. Kotkin, S.L. Panfil, V.G. Serbo, V.I. Telnov, Nucl. Instrum. Methods A 219 (1984) 5.

[24] A. Zee, Phys. Lett. B 161 (1985) 141;
S. Kanemura, T. Kasai, G.L. Lin, Y. Okada, J.J. Tseng, C.P. Yuan, Phys. Rev. D 64 (2001) 053007, hep-ph/0011357;
L.M. Krauss, S. Nasri, M. Trodden, Phys. Rev. D 67 (2003) 085002, hep-ph/0210389;
K.S. Babu, E. Ma, Int. J. Mod. Phys. A 23 (2008) 1813, arXiv: 0708.3790 [hep-ph];
M. Aoki, S. Kanemura, O. Seto, arXiv: 0807.0361 [hep-ph].

[25] F. Cornet, W. Hollik, arXiv: 0808.0719 [hep-ph].